Electric Power Systems Research 47 (1998) 181–188

Limit cycles in power systems due to OLTC deadbands and load–voltage dynamics

Mats Larsson [a,*], Dragana H. Popović [b], David J. Hill [b]

[a] *Department of Industrial Electrical Engineering and Automation, Lund Institute of Technology, Box 118, S-221 00 Lund, Sweden*

[b] *Department of Electrical Engineering, University of Sydney, Sydney, NSW 2006, Australia*

Received 23 February 1998; accepted 30 March 1998

Abstract

In this paper, the phenomenon of limit cycle due to load–tap changer interaction is investigated. The role of OLTC deadband in creating a limit cycle phenomenon is addressed. The impact of tap dynamics modelling on system/voltage behaviour is carefully considered. Analytical insights into observed behaviour of power systems with different tap models are given using eigenvalue analysis, the describing function method and time simulation. The conditions for occurrence of limit cycles and the identification of key parameters influencing their characteristics are another important aspect of this investigation.

Keywords: Limit cycles; OLTC deadbands; Load–voltage dynamics

1. Introduction

Studies of serious contingencies and associated voltage instability problems during the past decade have revealed different mechanisms underlying these events. Voltage misbehaviour has been shown as not necessarily just monotonic, influencing researchers to investigate various potential sources of the system oscillatory behaviour. This paper further explores the oscillatory behaviour of power supply systems with emphasis on illustrating interactions between on-load tap changer (OLTC) and load dynamics.

OLTCs have been shown to play an important role in long term voltage collapse [1], since they aim to keep load voltages, and therefore the load power constant, even though transmission system voltages may be reduced. Considerable effort has been given to voltage behaviour research indicating that the dynamics of voltage collapse are closely linked to dynamic interaction between the OLTCs and loads. It led to significant progress in the area of dynamic load modelling. However, dynamic modelling of OLTCs received little attention over the past decade. An early detailed description of a typical OLTC control system was given in [2]. The proposed OLTC model was a complex non-linear dynamic model that encompassed some inherent time delays. Recent work presented in [3] further explored the tap changer modelling issue. Depending on the OLTC characteristic (type of time delay), various discrete state dynamic models and corresponding continuous approximations were derived. However, most of the power system dynamic studies so far have used quite simplified OLTC representations. The main focus of these studies, which mainly relate to voltage stability questions, has been on understanding the complex dynamic nature of voltage collapse, to which OLTC dynamics significantly contributes. The role of OLTCs in combination with aggregate loads has received considerable attention [4–8]. Voltage instability problems concerned with OLTC dynamics were analysed in [4,5,7,8] using the continuous state OLTC model. Stability conditions providing proper coordination of multiple OLTCs were derived in [6,9] using a discrete state tap model. Limit cycles and other oscillatory voltage instability problems created by interaction between cascaded tap changing transformers and/or by load–tap interaction were investigated in [10–12].

In this paper, the influence of OLTC modelling in a power system loaded close to oscillatory voltage instability is studied. The OLTC deadband is shown to play

* Corresponding author. Fax: +46 46 142114.

0378-7796/98/$19.00
PII S0378-7796(98)00062-5

a central role in creating a limit cycle phenomenon. Using the describing function method, the conditions for this phenomenon to appear is derived.

2. Example system

A single load, single OLTC system such as shown in Fig. 1 is considered. The example system represents a distribution bus fed through a tap changing transformer and a transmission system equivalent. To increase transfer limits, the distribution system has been compensated by a capacitor bank. Although simple, the system contains all the principal components that affect voltage behaviour, especially after line fault or under heavy load conditions.

2.1. Load and network models

Focusing on tap changer dynamics, and therefore on a slower time scale (below ≈ 0.1 Hz) than the one relevant to generator dynamics, the generator bus is modelled as an infinite bus. The load is modelled as an exponential recovery load according to [13]:

$$\dot{x}_{\mathrm{p}} = \frac{1}{T_{\mathrm{p}}}(-x_{\mathrm{p}} + P_{\mathrm{s}}(V) - P_{\mathrm{t}}(V)) \tag{1}$$

$$P_d = x_{\mathrm{p}} + P_{\mathrm{t}}(V), \tag{2}$$

where $P_{\mathrm{s}}(V) = kP_0 V^{\alpha_{\mathrm{s}}}$ is the steady-state and $P_{\mathrm{t}}(V) = kP_0 V^{\alpha_{\mathrm{t}}}$ the transient voltage dependency. P_d is the actual active load power and T_{p} is the active power recovery time constant. For the reactive load power, a similar model is used with corresponding characteristics $Q_{\mathrm{s}}(V) = kQ_0 V^{\beta_{\mathrm{s}}}$, $Q_{\mathrm{t}}(V) = kQ_0 V^{\beta_{\mathrm{t}}}$ and time constant T_{q}. The transformer is modelled as a pure reactance in series with an ideal transformer. The parameter k has been introduced as a scale factor on the load parameters P_0, Q_0 and B_0.

Combining the load dynamics with power balance equations at the load bus, the model can be written in the differential–algebraic (DA) form

$$\dot{x} = f(\boldsymbol{x}, \boldsymbol{V}) \tag{3}$$

$$0 = g(\boldsymbol{x}, \boldsymbol{V}, n) \tag{4}$$

where $\boldsymbol{x} = [x_{\mathrm{p}}, x_{\mathrm{q}}]^T$ is the load state vector, $\boldsymbol{V} = [v, \delta]^T$ is the load voltage vector and n is the transformer tap ratio. For the example system, functions f and g can be written as

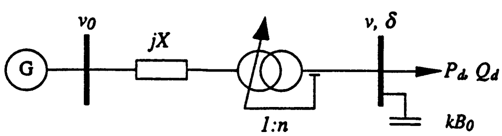

Fig. 1. Example power system studied.

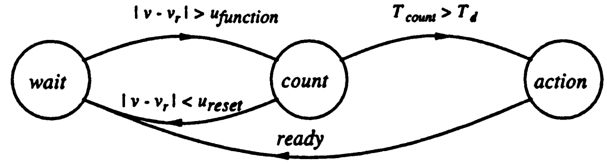

Fig. 2. State graph illustrating function of a non-sequential OLTC control system.

$$f(\boldsymbol{x}, \boldsymbol{V}) = \begin{bmatrix} \dfrac{1}{T_{\mathrm{p}}}(-x_{\mathrm{p}} + kP_0(v^{\alpha_{\mathrm{s}}} - v^{\alpha_{\mathrm{t}}})) \\ \dfrac{1}{T_{\mathrm{q}}}(-x_{\mathrm{q}} + kQ_0(v^{\beta_{\mathrm{s}}} - v^{\beta_{\mathrm{t}}})) \end{bmatrix} \tag{5}$$

$$g(\boldsymbol{x}, \boldsymbol{V}, n) = \begin{bmatrix} \dfrac{v\,\sin(\delta)v_0}{Xn} + x_{\mathrm{p}} + kP_0 v^{\alpha_{\mathrm{t}}} \\ \dfrac{V(V - \cos(\delta)v_0 n)}{Xn^2} + x_{\mathrm{p}} kQ_0 v^{\beta_{\mathrm{t}}} - kB_0 v^2 \end{bmatrix} \tag{6}$$

2.2. OLTC models

The conventional OLTC control is a simple incremental control with a time delay and a deadband. The size of the dead zone sets the tolerance for long term voltage deviations and the time delay is primarily intended for noise rejection. Detailed descriptions of OLTC control systems can be found in [2,3].

The typical non-sequential OLTC control system can be modelled by the state graph of Fig. 2. The system remains in the state *wait* while the voltage deviation ($|v - v_{\mathrm{r}}|$) is less than the function voltage (u_{function}). When the limit is exceeded, a transition to the state *count* occurs. Upon entering *count*, a timer is started and is kept running until either it reaches the delay time T_{d}, causing a transition to the state *action*, or if the voltage deviation becomes less than the reset voltage (u_{reset}), firing a transition to the state *wait* and reset of the timer. When entering the state *action*, a control pulse to operate the tap changer is given. After the mechanical delay time (T_{m}), the tap operation is completed. The control system then receives a ready signal from the tap changer and returns to state *wait*. The time delay is tuned by the time delay constant T_{d0}. The actual time delay can then be either fixed ($T_{\mathrm{d}} = T_{\mathrm{d0}}$) or inversely proportional to the voltage deviation ($T_{\mathrm{d}} \sim T_{\mathrm{d0}}/|v - v_{\mathrm{r}}|$).

For agreement with [3], function and reset voltages have been chosen to be identical ($u_{\mathrm{function}} = u_{\mathrm{reset}} = \mathrm{DB}/2$). Possible tap ratio change is typically ± 10–15% in steps of 0.6–2.5%. Typical setting of delay times (T_{d}) is in the range 30–120 s, whilst the deadband (DB) is usually chosen slightly smaller than two tap steps. The mechanical delay time (T_{m}) is usually in the range 1–5 s.

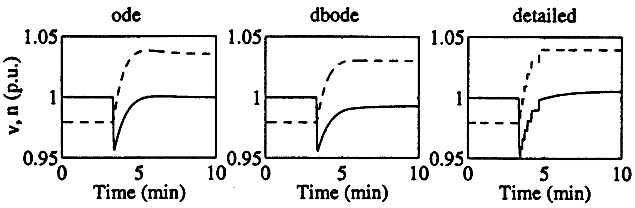

Fig. 3. Response to voltage disturbance for the three OLTC models—load side voltage (solid line) and tap ratio (dashed line).

Several models with different types of time delay are given in [3]. Here, for the purpose of studying the limit cycling phenomenon, we will restrict our attention to the following three OLTC models:

ODE. This is a model often used in voltage stability analysis. It approximately describes the dynamics of an OLTC with an inverse time delay characteristic, but does not account for the deadband or discrete tap steps. The model can be written as

$$\frac{\mathrm{d}n}{\mathrm{d}t} = -\frac{1}{T}(v - v_r) \tag{7}$$

where v is the regulated voltage, v_r is the voltage setpoint and T is the controller time delay.

DBODE. Augmenting the ODE model with a deadband on the input we get

$$\frac{\mathrm{d}n}{\mathrm{d}t} = \begin{cases} -\frac{1}{T}(v - v_r - \mathrm{DB}/2) & \text{if } v - v_r > \mathrm{DB}/2 \\ -\frac{1}{T}(v - v_r + \mathrm{DB}/2) & \text{if } v - v_r < -\mathrm{DB}/2 \\ 0 & \text{if } |v - v_r| < \mathrm{DB}/2 \end{cases} \tag{8}$$

where DB is the size of the deadband.

Detailed is the control system described by Fig. 2, with $T_d = \mathrm{DB}T_{d0}/(2|v - v_r|)$ and $T_m = \mathrm{DB}T_{m0}/(2|v - v_r|)$.

It is shown in [3] that if T in Eq. (7) is chosen such that T (DB/2)/tap step $= T_{d0} + T_{m0}$, the ODE model makes the best continuous state match to the Detailed model in the sense of time response.

To illustrate potential differences in OLTC responses (Fig. 3), a 5% disturbance in the feeding voltage, v_0, is assumed in the moderately loaded ($k = 0.5$) power system of Fig. 1. System parameter values are given in Table 1. With the ODE model, the tap ratio is adjusted until the voltage deviation becomes exactly zero. Since at that time, the load dynamics have not settled yet, there is a slight overshoot. With the DBODE model, the feedback path is broken as soon as the voltage deviation is within the deadband. Therefore, overshoot due to the load dynamics is avoided. With the Detailed model, the tap state is changed in fixed steps. Additional voltage restoration due to load dynamics following the last tap operation is also present with this model.

Despite the slight differences in responses in Fig. 3, the overall behaviour of the moderately loaded system is similar for all OLTC models. The sensitivity to the OLTC modelling is however more significant in a heavily loaded power system. As it will be shown in the following sections, the occurrence of voltage collapse or limit cycles is greatly affected by the OLTC model used in the analysis.

3. Small signal stability analysis

The system equilibrium can be found by solving the equations $f(\boldsymbol{x}, \boldsymbol{V}) = g(\boldsymbol{x}, \boldsymbol{V}, n) = 0$ for the unknowns $\boldsymbol{x}$, n and δ. Linearising Eqs. (3) and (4) around the equilibrium point yields

$$\frac{\mathrm{d}(\Delta \boldsymbol{x})}{\mathrm{d}t} = \frac{\partial f}{\partial \boldsymbol{x}}\Delta \boldsymbol{x} + \frac{\partial f}{\partial \boldsymbol{V}}\Delta \boldsymbol{V} \tag{9}$$

$$0 = \frac{\partial g}{\partial \boldsymbol{x}}\Delta \boldsymbol{x} + \frac{\partial g}{\partial \boldsymbol{V}}\Delta \boldsymbol{V} + \frac{\partial g}{\partial n}\Delta n \tag{10}$$

Eliminating $\Delta \boldsymbol{V}$ from Eq. (9), the linearised system model can be written in the standard state space form with Δn as an input and $\Delta \boldsymbol{V}$ as an output. That is,

$$\frac{\mathrm{d}(\Delta \boldsymbol{x})}{\mathrm{d}t} A\Delta \boldsymbol{x} + B\Delta n \tag{11}$$

$$\Delta \boldsymbol{V} = C\Delta \boldsymbol{x} + D\Delta n \tag{12}$$

where $A = (\partial f/\partial \boldsymbol{x}) - \partial f/\partial \boldsymbol{V}(\partial g/\partial \boldsymbol{V})^{-1}(\partial g/\partial \boldsymbol{x})$, $B = -\partial f/\partial \boldsymbol{V}(\partial g/\partial \boldsymbol{V})^{-1}(\partial g/\partial n)$, $C = -(\partial g/\partial \boldsymbol{V})^{-1}(\partial g/\partial \boldsymbol{x})$ and $D = -(\partial g/\partial \boldsymbol{V})^{-1}(\partial g/\partial n)$. The state space form has the more convenient transfer function equivalent

Table 1
Network, load and OLTC parameters

Network data	X	B_0				
	0.5	0.5				
Load data	P_0	Q_0	$T_p = T_q$	$\alpha_s = \beta_s$	$\alpha_t = \beta_t$	
	1.0	0.5	60	0	2	
OLTC	Tap step	Tap limits	DB/2	T	T_{d0}	T_{m0}
	1%	±15%	0.9%	30	25*(1/0.9)	5*(1/0.9)

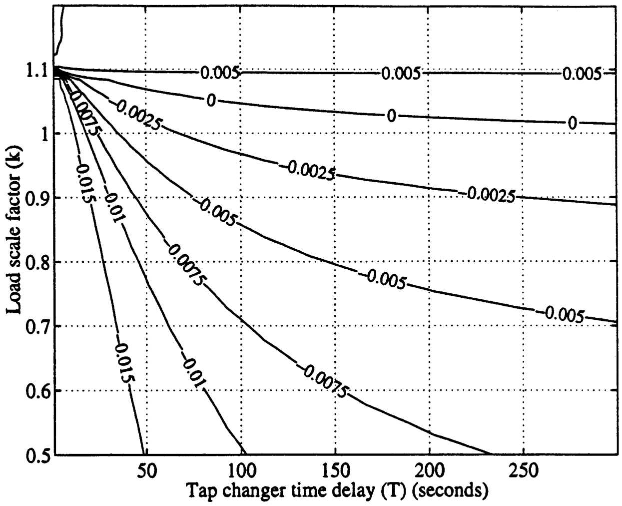

Fig. 4. Stability contours as a function of load factor (k) and OLTC time delay (T).

$$G_n(s) = C(sI - A)^{-1}B + D \tag{13}$$

By combining the ODE OLTC model with the linearised system model, small signal stability analysis is made using the parameter values given in Table 1. Fig. 4 shows a contour map of the real part of the dominant mode eigenvalue as a function of the OLTC time delay (T) and the load scale factor (k). The stability bound is thus given by the 0-contour. Two observations that can be made regarding the system small disturbance stability are as follows: first, for $T = 30$ s, the system is stable if $k < 1.082$, and second, for $k < 0.986$, the system is stable for all positive T.

In the next sections, these stability results will be verified by simulation.

4. Mechanisms in the limit cycle phenomenon

To illustrate the contributing mechanisms to the limit cycle phenomenon, a simulation is made using the Detailed OLTC model. The reactive load has been made over-compensated by setting $B_0 = 0.6$ pu. The other parameter values are as given in Table 1 and the load factor is set to $k = 1$.

Referring to the simulation results in Fig. 5, the course of events is as follows. Initially, the voltage deviation is positive and growing. When the deadband is exceeded, the timer is started. As soon as the timer expires, a tap operation is made and the new operating point is determined by the change in tap ratio, the change in reactive output from the capacitor bank and the instantaneous load relief according to $P_t(V)$. As the load recovers to the value dictated by $P_s(V)$, the load-side voltage decreases further, and consequently, decreases capacitor bank output too. If the capacitor bank and load recovery are sufficiently strong, as is the case here, the voltage continues to decrease until a reverse tap operation is executed.

Voltage then starts increasing due to the change in tap ratio, capacitor bank output and load response. The influence of the load dynamics is now opposite as compared with the downward tap operation, and voltage now increases until a new downward tap operation is necessary. The resulting cyclic behaviour is called a limit cycle.

From this simulation it is evident that a limit cycle results from an interaction between OLTC deadbands, OLTC and load dynamics accompanied by the load/capacitor voltage sensitivity.

Note however, that the instability observed in this example originates from the unstable load dynamics (including capacitor bank) and the interaction between load and tap changer. This indicates that it is not possible to avoid limit cycle behaviour just by retuning the OLTC deadbands or time delays. This issue will be further discussed in Section 5, where an analytical insight is given using the describing function method and time simulation.

5. Describing function analysis

The describing function method can be used to predict existence, period time and amplitude of limit cycles in linear systems under non-linear feedback, such as shown in Fig. 6(b). A thorough presentation of the describing function method, along with describing functions of some standard non-linearities, are given in [14].

The method is based on the assumption that since all limit cycles are periodic, they are approximately sinusoidal. This assumption is reasonable if the transfer function $G(s)$ in Fig. 6(b) has low pass characteristics, i.e. filters out higher-order harmonics. The linearised

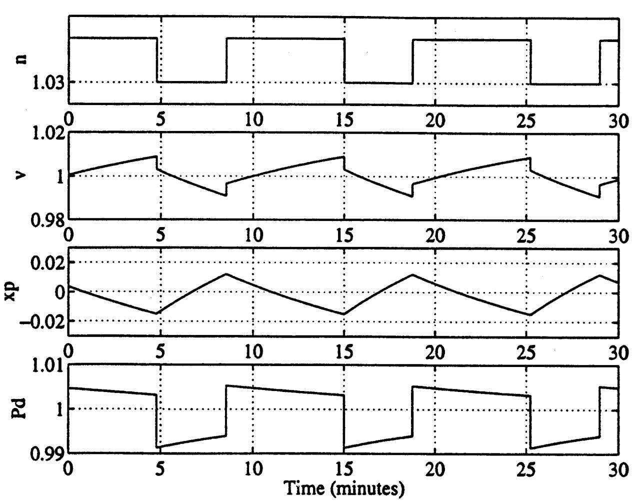

Fig. 5. Self-sustained oscillation.

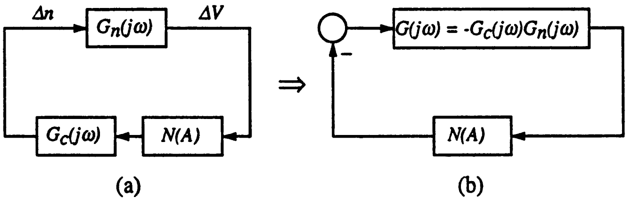

Fig. 6. Schematic of the feedback loop used in the describing function analysis.

model $G_n(s)$ given by Eq. (13) does not have this property (since the matrix D in Eq. (12) is non-zero). However when lumped with the ODE part of the DBODE model denoted by $G_c(s)$ in Fig. 6(a), it achieves this.

The describing function of the deadband in the DBODE model is [14]:

$$N(A) = \begin{cases} 1 - \frac{2}{\pi}\left(\sin^{-1}\left(\frac{\mathrm{DB}}{2A}\right) + \frac{\mathrm{DB}}{2A}\sqrt{1 - \left(\frac{\mathrm{DB}}{2A}\right)^2}\right) \\ \text{if } A > \mathrm{DB}/2 \\ 0 \quad \text{if } A < \mathrm{DB}/2 \end{cases} \tag{14}$$

where A is the amplitude of a sinusoidal input. A necessary condition for existence of a limit cycle is [14]:

$$G(j\omega) = -\frac{1}{N(A)} \tag{15}$$

This equation is not easily solved analytically in terms of load and OLTC model parameters, but can be solved graphically or numerically. A limit cycle exists for each intersection of the curves $G(j\omega)$ and $-1/N(A)$ in a Nichols diagram. From the point of intersection, the amplitude and frequency of the limit cycle are approximately determined.

In Fig. 7 the two curves are shown for different values of k in the interval [0.8, 1.1] and $T = 30$ s. The following three cases can be distinguished:

1. the open-loop system $G(s)$ has only stable poles, the closed-loop system is stable, the phase changes from $-90°$ at low frequencies to $-90°$ at high frequencies, no intersection can occur (dotted lines);
2. the open-loop system has one unstable pole, the closed-loop system is stable, the phase changes from $-270°$ at low frequencies to $-90°$ at high frequencies, one intersection (thin solid lines);
3. the open-loop system has one unstable pole, the phase changes from $-270°$ at low frequencies to $-90°$ at high frequencies, the closed-loop system experiences instability, no intersection (dash-dotted lines).

In case 2, the intersection indicates that a limit cycle exists. The amplitude of the limit cycle is determined by the curve $-1/N(A)$ which depends only on the deadband size and the frequency is determined from the curve $G(j\omega)$, which is independent of the deadband size. The describing function always maps on a line between ($0dB$, $-180°$) and (∞, $-180°$) regardless of the deadband size. It implies that a change in the deadband size does not affect the existence of a limit cycle. The change in time constants, such as time delay or load recovery time constants, affects $G_c(j\omega)$ as a gain factor, and therefore shifts the curve $G(j\omega)$ up or down in the Nichols plot. Consequently, the amplitude can be changed, but not the frequency. Shifting the curve below the point ($0dB$, $-180°$) could remove a limit cycle, but would also cause instability of the closed-loop system. Note however, that load scaling (k) and the voltage sensitivity parameters of the load have a significant influence, and can affect existence, frequency and amplitude of limit cycles, since they directly affect the shape and position of the curve $G(j\omega)$.

Simulation is used to verify the predictions of the existence and stability of limit cycles. Fig. 8 (top) illustrates the stable system behaviour for the lower bound on k ($k = 0.986$) along with the describing function analysis result, which correctly predicts that the system is free from limit cycles. Increasing the value of k yields limit cycles of various amplitudes. A_{lim} and T_{lim} given in the figure denote the amplitude and period time of limit cycle as predicted by the describing function method. As can be seen from Fig. 8, the limit cycle amplitude is predicted accurately for all values of k, but the frequency is not for small k. For $k = 1.09$, no limit cycle is present, but the closed-loop system is unstable as predicted by the small disturbance and describing function analysis. Note that for the describing function method to provide an accurate prediction of the limit cycle frequency, the two curves $G(j\omega)$ and $-1/N(A)$ should intersect at an angle as close as possible to 90°. Referring to Fig. 8, it is clear that for the smaller values of k, the angle of intersection deviates increasingly from the ideal 90°. The logarithmic scale of the y-axis partly conceals this deviation in Fig. 8.

6. Comparison of OLTC models

In this section the sensitivity of system behaviour to OLTC modelling is investigated for a highly loaded power system. Fig. 9 presents simulation results obtained with $k = 1$ and $T = 30$ s. As seen in the figure, the system exhibits stable behaviour with the ODE model. This is in agreement with small-disturbance stability analysis. For the models that contain the deadband though, there are limit cycles with an amplitude of 0.01 pu and different frequencies, depending on the OLTC model used. The small disturbance analysis in Section 3 also indicates, that the system with the ODE model is unstable if the load dynamics is sufficiently

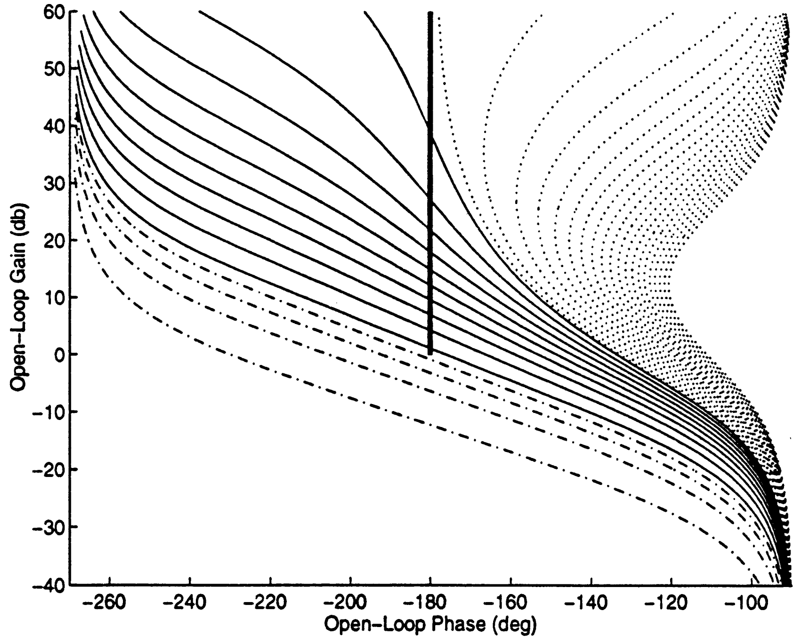

Fig. 7. Nichols diagram of $G(j\omega)$ for different values of k in the interval [0.8, 1.1] ($T = 30$ s). The thick line is $-1/N(A)$.

fast compared with the OLTC time delay. This is illustrated in Fig. 10 (top left) for $k = 1$, $T = 120$ s and $T_p = T_q = 10$ s. The system remains unstable with the DBODE model too, but the extra lag introduced by the deadband causes the oscillations to grow more rapidly and voltage collapse occurs one period earlier for that model than for the ODE model. However, with the Detailed model, the system exhibits a limit cycle preventing the occurrence of oscillatory voltage instability.

From the simulations in this section, we see that the modelling of the OLTC has a significant effect on the behaviour of the system model.

7. Discussion

The describing function analysis results in terms of conditions for limit cycle existence, presented in Section 5, are valid only for the DBODE OLTC model. Nevertheless, the analysis has clearly shown that the limit cycle phenomena are related to the load dynamics, deadbands and the interaction between load and tap changer. It has also been shown that the limit cycles are present in the mathematical model of the power system and not due to numerical problems in the simulation. A similar analysis for the Detailed OLTC model is possible but would require a derivation of the describing functions corresponding to the non-linearities present in that model. Note that, since these non-linearities have memory, the describing functions will be frequency-dependent as well as amplitude-dependent.

Because of the well-known limitations of the describing function method [14], only a single load, single OLTC system has been considered here. However, the simulation of a power system model with cascaded OLTCs has been shown to exhibit a similar or even greater tendency to self-oscillate [10,11].

A somewhat surprising conclusion made in the paper is that the limit cycles cannot necessarily be avoided by adjusting the OLTC deadband or time delay. The explanation is that when the voltage deviation is within the deadband, the system effectively operates in open-loop. As soon as the deadband is exceeded, the control loop is closed again and the instability is arrested. Referring to Fig. 7, a necessary condition for the limit cycle to appear is that the open-loop system is unstable (due to capacitor bank and load dynamics interaction). If that is the case, an increase of the deadband size will only increase the amplitude of a limit cycle but will not remove it. Similarly, the different time delays in the OLTC control system have no influence on the existence of limit cycles, only on the amplitude and period time. The only parameters which can affect the existence of limit cycles are load and network parameters. Note that for the sake of getting more insights into the role of deadbands and load–tap interaction in creating the cyclic behaviour, the tap limits were turned off in our study. That potential source of limit cycles is illustrated in [12].

Despite the lack of clear evidence for the deadband and load-tap interaction related limit cycles occurring in power systems, the analysis presented in the paper offers an analytical study that clearly illustrates the potential for this sort of phenomena arising in non-linear, highly stressed power systems.

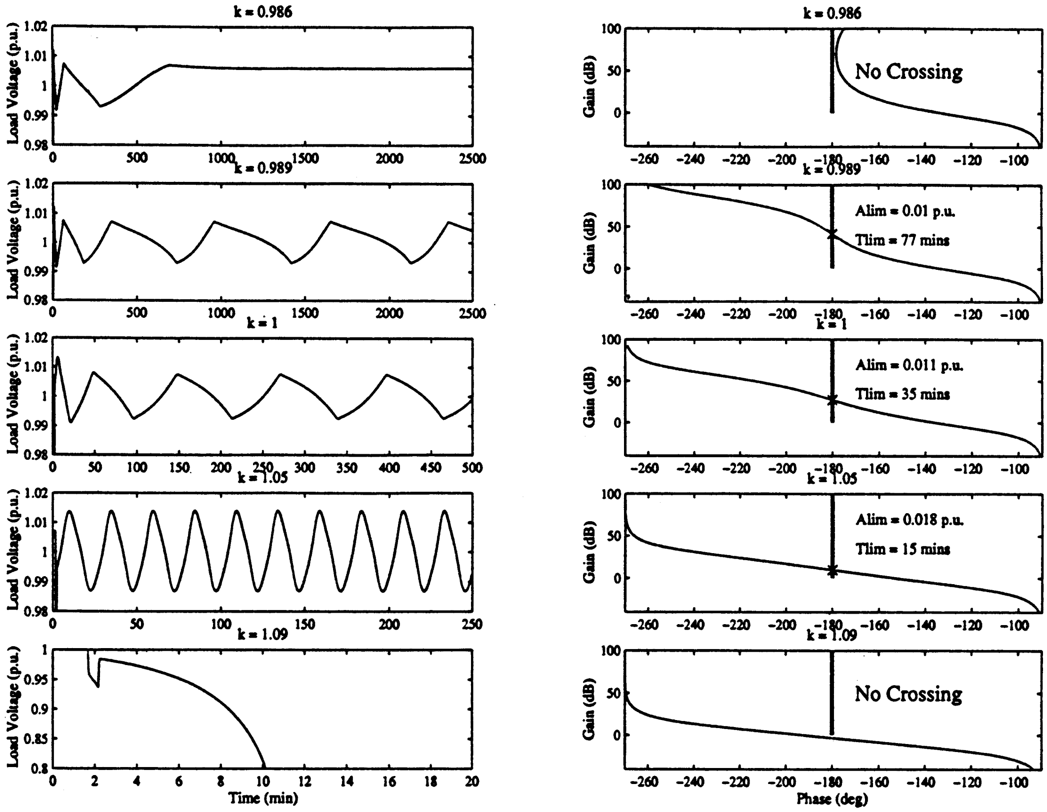

Fig. 8. Simulations and describing function analysis with different k, ($T = 30$ s, DBODE model).

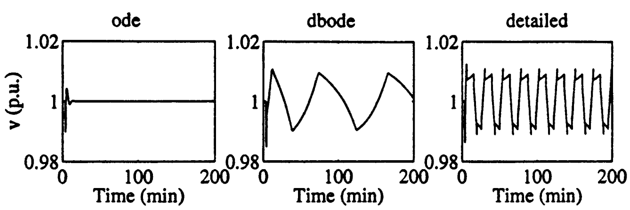

Fig. 9. Simulations of feeding voltage disturbance for different OLTC models; $k = 1$, $T = 30$ s.

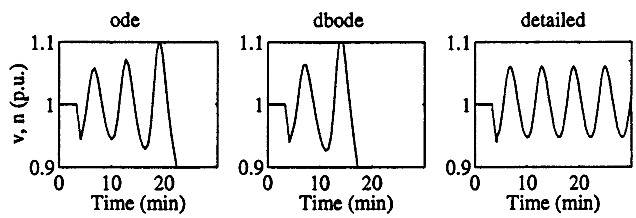

Fig. 10. Simulations of feeding voltage disturbance for different OLTC models; $k = 1$, $T = 120$ s, $T_p = 10$ s, $T_q = 10$ s.

8. Conclusions

In this paper the phenomenon of limit cycle behaviour due to tap changer deadbands and load–tap interaction has been investigated. The effect of tap dynamics modelling on system behaviour is illustrated. It has been shown that the results from small disturbance analysis based on a continuous OLTC model are unreliable, especially in a heavily loaded power system. Under heavy load conditions, the system with a detailed OLTC model exhibits a limit cycle that will arrest oscillatory voltage instability predicted by small disturbance analysis.

The key parameters in creating/avoiding this kind of limit cycles are identified as the system load level, degree of reactive compensation and the load voltage dependency. In certain loading conditions, adjusting OLTC control system parameters such as time delays or deadband size is shown not to have any effect on the existence of the limit cycles.

Acknowledgements

This work was sponsored by a grant from Sydkraft AB, Sweden and Elforsk, Sweden and by an Australian Electricity Supply Industry Research Board project grant 'Voltage Collapse Analysis and Control'.

References

[1] K. Walve, Modelling of power system components at severe disturbances, CIGRÉ, Paper 38-18, 1986.

[2] M.S. Ćalović, Modelling and analysis of underload tap-changing transformer control system, IEEE Trans. Power Apparat. Syst. 103 (1984) 1909–1915.
[3] P.W. Sauer, M.A. Pai, A comparison of discrete vs. continuous dynamic models of tap-changing-under-load transformers, in: Proc. NSF/ECC Workshop on Bulk power System Voltage Phenomena III: Voltage Stability, Security and Control, Davos, Switzerland, 1994.
[4] S. Abe, Y. Fukunaga, A. Isono, B. Kondo, Power system voltage stability, IEEE Trans. Power Apparat. Syst. 101 (1982) 3830–3840.
[5] C.C. Liu, K.T. Vu, Analysis of tap-changer dynamics and construction of voltage stability regions, IEEE Trans. Circuits Syst. 36 (1989) 575–590.
[6] J. Medanić, M. Ilić-Spong, J. Christensen, Discrete models of slow voltage dynamics for under load tap-changing transformer coordination, IEEE Trans. Power Syst. 2 (1987) 873–882.
[7] D.H. Popović, I.A. Hiskens, D.J. Hill, Investigations of load–tap changer interaction, Int. J. Electr. Power Energy Syst. 18 (2) (1996) 81–97.
[8] K.T. Vu, C.C. Liu, Shrinking stability regions and voltage collapse in power systems, IEEE Trans. Circuits Syst. I: Fund. Theory Appl. 39 (1992) 271–289.
[9] N. Yorino, M. Danyoshi, M. Kitagawa, Interaction among multiple controls in tap change under load transformers, IEEE/PES Winter Meeting, 1996. Publication 96 WM 310-3 PWRS.
[10] I.A. Hiskens, D.J. Hill, Dynamic interaction between tapping transformers, Proc. 11th Power Systems Computation Conference, Avignon, France, September 1993.
[11] D.H. Popović, D.J. Hill, I.A. Hiskens, Oscillatory behaviour of power supply systems with single dynamic load, Proc. 12th Power Systems Computation Conference, August 1996.
[12] C.D. Vournas, T.V. Cutsem, Voltage oscillations with cascaded load restoration, Proc. IEEE/KTH Stockholm PowerTech Conference, 1995. Publication SPT PS 22-04-0426.
[13] D. Karlsson, D.J. Hill, Modelling and identification of nonlinear dynamic loads in power systems, IEEE Trans. Power Syst. 9 (1994) 157–163.
[14] J.C. Hsu, A.U. Meyer, Modern Control Principles and Applications, McGraw-Hill, New York, 1968.